

## One-step preparation of reduction-responsive poly(ethylene glycol)-poly(amino acid)s nanogels as efficient intracellular drug delivery platforms†

Jianxun Ding,<sup>‡ac</sup> Fenghua Shi,<sup>‡ab</sup> Chunsheng Xiao,<sup>ac</sup> Lin Lin,<sup>a</sup> Li Chen,<sup>\*b</sup> Chaoliang He,<sup>a</sup> Xiuli Zhuang<sup>\*a</sup> and Xuesi Chen<sup>a</sup>

Received 12th August 2011, Accepted 15th September 2011

DOI: 10.1039/c1py00360g

A series of disulfide-core-cross-linked poly(ethylene glycol)-poly(amino acid)s star copolymers were synthesized through one-step ring-opening polymerization of L-phenylalanine *N*-carboxyanhydride (L-Phe NCA) and L-cystine *N*-carboxyanhydride (L-Cys NCA) with amino group terminated poly(ethylene glycol) monomethyl ether (mPEG-NH<sub>2</sub>) as macroinitiator. The reduction-responsive PEG-poly(amino acid)s nanogels (NGs) were prepared by directly dispersing the resultant PEG-poly(amino acid)s in phosphate buffer solution at pH 7.4. Dynamic light scattering (DLS) measurements showed that the reducible NG swelled in response to 10 mM glutathione (GSH). Doxorubicin (DOX), an anthracycline anticancer drug, was loaded into the NGs. The *in vitro* release results revealed that the release behaviors could be adjusted by GSH concentration, and poly(amino acid)s content and composition. The intracellular DOX release results showed that enhanced intracellular DOX release occurred in GSH pretreated Henrietta Lacks (HeLa) cells. *In vitro* methyl thiazolyl tetrazolium (MTT) assays indicated that the NGs were biocompatible, and DOX-loaded NG showed higher cellular proliferation inhibition towards GSH pretreated HeLa cells than that of non-pretreated cells. Therefore, the NGs can efficiently deliver anticancer drugs into tumor cells and inhibit cell proliferation, rendering highly promising for targeted intracellular delivery of operative chemotherapeutic drugs in cancer therapy.

### Introduction

Up to now, despite the fact that many anticancer drugs (*e.g.* doxorubicin (DOX), paclitaxel (PTX), and chlorambucil) for cancer chemotherapy have been developed, the clinical outcomes are dissatisfactory because of the life-threatening side effects, such as leukaemia and cardiotoxicity.<sup>1–3</sup> To reduce or minimize these side effects, various nanocarriers, such as polymeric micelles,<sup>4–7</sup> vesicles,<sup>8,9</sup> liposomes<sup>10</sup> and nanogels,<sup>11–15</sup> have been developed for delivery of drugs. Among all of the aforementioned nanovehicles, stimuli-responsive drug delivery systems, especially releasing drugs triggered by intracellular stimuli, such as pH,<sup>16–20</sup>

temperature,<sup>16,18</sup> redox,<sup>21–23</sup> enzymes<sup>9,24</sup> *etc.*, have been considered as attractive potential carriers. As soon as they reach the targeted tumor sites, the smart nanocarriers can rapidly enter cells through endocytosis and fast drug release is triggered by the intracellular stimuli, thus resulting in aggressive activity toward tumor cells and maximal chemotherapeutic efficacy with fewer side effects.<sup>3,19</sup>

Reduction-responsive nanocarriers containing disulfide bonds have received considerable attention for intracellular drug delivery due to the difference in the redox potential between the mildly oxidizing extracellular milieu and the reducing intracellular environment.<sup>1</sup> The disulfide bonds can be reductively degraded in presence of glutathione (GSH), a thiol-containing tripeptide. The intracellular concentration of GSH is ~10 mM and significantly higher than that outside cells (~2 μM).<sup>23</sup> Furthermore, the GSH concentration in some tumor cells (*e.g.* human lung adenocarcinoma A549 cells) has been reported to be several times higher than that in the normal cells.<sup>25</sup> The dramatic variation of the GSH concentration can provides an opportunity for designing intracellular specific drug delivery systems. Thus, such smart nanovehicles containing GSH-cleavable disulfide bonds may hold vast potential for efficient intracellular release of anticancer drugs.

In the present work, the reduction-responsive PEG-poly(amino acid)s nanogels (NGs) were developed as a novel platform for rapid intracellular drug release with destruction of the

<sup>a</sup>Key Laboratory of Polymer Ecomaterials, Changchun Institute of Applied Chemistry, Chinese Academy of Sciences, Changchun, 130022, P. R. China. E-mail: zhuangxl@ciac.jl.cn; Fax: +86-431-85262367; Tel: +86-431-85262367

<sup>b</sup>Department of Chemistry, Northeast Normal University, Changchun, 130022, P. R. China. E-mail: chenl686@nenu.edu.cn; Fax: +86-431-85262367; Tel: +86-431-85262367

<sup>c</sup>Graduate University of the Chinese Academy of Sciences, Beijing, 100039, P. R. China

† Electronic supplementary information (ESI) available: <sup>1</sup>H NMR spectrum of mPEG-NH<sub>2</sub>, and fluorescence measurements of NGs with pyrene as probe. See DOI: 10.1039/c1py00360g

‡ These authors contributed equally to this paper.

disulfide bonds in presence of the intracellular GSH. Currently, the NGs satisfying both the requirements of enhanced structural stability and cell-specific drug releasing property have been recognized as powerful vehicles for intracellular drug delivery.<sup>26,27</sup> In this work, poly(ethylene glycol) (PEG) and poly(amino acid)s are selected as building components for NGs due to their good biocompatibility.<sup>28,29</sup> First, a series of novel reduction-responsive NGs were prepared through one-step ring-opening polymerization (ROP) of L-Phe NCA and L-Cys NCA with mPEG-NH<sub>2</sub> as macroinitiator, and followed by dispersing the obtained PEG-poly(amino acid)s in phosphate buffer solution (PBS) at pH 7.4. Doxorubicin (DOX), an anthracycline anticancer drug, has been loaded into NGs, and the release behaviors of DOX from NGs depended on GSH concentration, and poly(amino acid)s content and composition. The GSH-mediated intracellular drug delivery was also investigated against HeLa cells by pretreating these cells with GSH, which could increase the intracellular GSH concentration. These novel reducible NGs are highly promising for the targeted intracellular delivery of anticancer drugs.

## Experimental section

### Materials

L-phenylalanine and L-cystine were purchased from GL Biochem (Shanghai) Co., Ltd. L-phenylalanine *N*-carboxyanhydride (L-Phe NCA) was synthesized as described in our previous work.<sup>30</sup> Poly(ethylene glycol) monomethyl ether (mPEG,  $M_n = 5000$ ) was purchased from Aldrich and used without further purification. The amino group terminated poly(ethylene glycol) monomethyl ether (mPEG-NH<sub>2</sub>) was synthesized according to the literature procedure.<sup>31</sup> GSH (used for cell culture) and doxorubicin hydrochloride (DOX·HCl) were purchased from Aladdin Reagent (Shanghai) Co., Ltd. and Zhejiang Hisun Pharmaceutical Co., Ltd., respectively. Tetrahydrofuran (THF) was refluxed with sodium and distilled under nitrogen prior to use. *N,N*-Dimethylformamide (DMF) was stored over calcium hydride (CaH<sub>2</sub>) and purified by vacuum distillation with CaH<sub>2</sub>. All the other reagents and solvents were purchased from Sino-pharm Chemical Reagent Co., Ltd., China and used as obtained.

### Synthesis of L-cystine *N*-carboxyanhydride (L-Cys NCA)

L-Cys NCA was synthesized according to our previous work with slight modification (Scheme 1).<sup>28</sup> L-cystine (10.0 g, 41.6 mmol) and triphosgene (12.3 g, 41.6 mmol) were suspended in 200 mL of dry THF bubbled with slow steady nitrogen flux in a flame-dry three neck flask. The mixture was stirred at 60 °C until the cloudy solution turned clear within 3 h. After stirring at room temperature for further 30 min, the product was precipitated by excessive *n*-hexane and then purified by recrystallization thrice with THF and *n*-hexane (yield: 20%).



**Scheme 1** Synthesis pathway for L-Cys NCA.

### Preparation of disulfide-core-cross-linked PEG-poly(amino acid)s NGs

The disulfide-core-cross-linked PEG-poly(amino acid)s star copolymers were synthesized through one-step ROP of L-Phe NCA and L-Cys NCA with mPEG-NH<sub>2</sub> as macroinitiator (Scheme 2). Typically, L-Phe NCA (841.2 mg, 4.4 mmol), L-Cys NCA (350.7 mg, 1.2 mmol) and mPEG-NH<sub>2</sub> (1.0 g, 0.2 mmol) were dissolved in 15 mL of dry DMF in a flame-dry flask. The polymerization was performed at 25 °C for 3 d. Then, the solution was precipitated into excessive diethyl ether. The obtained product was further washed twice with diethyl ether and dried under vacuum at room temperature for 24 h (Yield: 88.7%). The disulfide-core-cross-linked PEG-poly(amino acid)s NGs were prepared by directly dispersing the resultant products in PBS at pH 7.4.

### Characterizations

The contents of carbon, hydrogen and nitrogen elements of NGs were estimated by elemental analysis (Vario EL III, Germany). <sup>1</sup>H NMR and <sup>13</sup>C NMR spectra were recorded on a Bruker AV 400 NMR spectrometer in dimethyl sulfoxide-*d*<sub>6</sub> (DMSO-*d*<sub>6</sub>) or trifluoroacetic acid-*d* (CF<sub>3</sub>COOD). FT-IR spectra were recorded on a Bio-Rad Win-IR instrument using the potassium bromide (KBr) method. Dynamic laser scattering (DLS) measurements were performed on a WyattQELS instrument with a vertically polarized He-Ne laser (DAWN EOS, Wyatt Technology). The scattering angle was fixed at 90°. Transmission electron microscopy (TEM) measurements were performed on a JEOL JEM-1011 transmission electron microscope with an accelerating voltage of 100 KV. A drop of the NG solution (0.05 g L<sup>-1</sup>) was deposited onto a 230 mesh copper grid coated with carbon and allowed to dry in air at 25 °C before measurements. The excitation spectra of pyrene were measured on a Perkin-Elmer LS50B luminescence spectrometer at the detection wavelength ( $\lambda_{em}$ ) of 390 nm.

### *In Vitro* drug loading and release

NG (25.0 mg), DOX·HCl (5.0 mg), and triethylamine (0.9 mg) were mixed in 3.0 mL of DMF. The mixture was allowed to stand at room temperature for 2 h. Then, 2 mL of deionized water was added dropwise to the solution under stirring. The mixture was stirred at room temperature for 6 h and the organic solvent was removed by dialysis against deionized water for 24 h to obtain the DOX-loaded NG. The solution was filtered and freeze-dried. The drug loading content (DLC%) and the drug loading efficiency (DLE%) of DOX-loaded NG were calculated by the following equations:

$$\text{DLC}\% = \frac{\text{amount of drug in NG}}{\text{amount of drug-loaded NG}} \times 100\%$$

$$\text{DLE}\% = \frac{\text{amount of drug in NG}}{\text{total amount of loaded drug}} \times 100\%$$

*In vitro* DOX release behaviors from the DOX-loaded NG were investigated in PBS at pH 7.4. The weighed freeze-dried DOX-loaded NG was suspended in 5 mL of PBS with 0, 2.5, 5 or



**Scheme 2** Schematic illustration of preparation, and drug loading and intracellular release of PEG-poly(amino acid)s NGs.

10 mM GSH and introduced into a dialysis bag (MWCO 3500 Da). The release experiment was initiated by placing the end-sealed dialysis bag into 50 mL of PBS with 0, 2.5, 5 or 10 mM GSH at 37 °C with continuous shaking at 70 rpm. At predetermined intervals, 2 mL of external release medium was taken out and the volume withdrawn was replenished with an equal volume of fresh release medium. The amount of released drug was assayed by spectrophotometry at 480 nm using the standard curve method.

### Intracellular drug release

The cellular uptake and intracellular release behaviors of DOX-loaded NGs were determined by confocal laser scanning microscopy (CLSM) toward HeLa cells. The cells were seeded in 6-well plates with a density of  $\sim 200\,000$  cells per well in 2 mL of complete DMEM and cultured for 24 h, and then treated with GSH (used for cell culture) for 2 h. Cells were washed by PBS and incubated at 37 °C for additional 0.5 or 2 h with DOX-loaded NG at a final DOX concentration of  $10\text{ mg L}^{-1}$  in complete DMEM. Cells without GSH treatment were used as the control. Then the culture medium was removed and cells were washed with PBS thrice. Thereafter, the cells were fixed with 4% formaldehyde for 30 min at room temperature, and the cell nuclei were stained with 4',6-diamidino-2-phenylindole (DAPI, blue). CLSM images of cells were obtained through confocal microscope (Olympus FluoView 1000).

### Cell viability assays

The relative cytotoxicities of NGs and DOX-loaded NG were assessed with MTT assays against HeLa cells. The cells were seeded in 96-well plates at  $\sim 20\,000$  cells per well in 100  $\mu\text{L}$  of complete DMEM containing 10% fetal bovine serum, supplemented with 50  $\text{U mL}^{-1}$  penicillin and 50  $\text{U mL}^{-1}$  streptomycin, and incubated at 37 °C in 5%  $\text{CO}_2$  atmosphere for 24 h, followed by removing culture medium and adding NGs solutions at

different concentrations (0 to  $50\text{ mg L}^{-1}$ ) or DOX-loaded NG (0 to  $10\text{ mg L}^{-1}$  DOX) ( $100\ \mu\text{L}$  in complete DMEM medium). The cells were subjected to MTT assay after being incubated for another 24 h. The absorbency of the solution was measured on a Bio-Rad 680 microplate reader at 490 nm. Cell viability (%) was calculated based on the following equation:  $(A_{\text{sample}}/A_{\text{control}}) \times 100$ , where  $A_{\text{sample}}$  and  $A_{\text{control}}$  denote the absorbencies of the sample and control wells, respectively.

## Results and discussion

### Synthesis and characterization of NGs

The poly(amino acid)s can be synthesized by the ROP of amino acid *N*-carboxyanhydride (NCA) monomers with primary amine as the initiator in a controlled way.<sup>32,33</sup> In this work, the disulfide-core-cross-linked PEG-poly(amino acid)s star copolymers were synthesized through one-step ROP of L-Phe NCA and L-Cys NCA with mPEG-NH<sub>2</sub> as macroinitiator in DMF at 25 °C, as shown in Scheme 2. Firstly, the novel L-Cys NCA was synthesized with the convenient synthetic route shown in Scheme 1. <sup>1</sup>H NMR (Fig. 1A), <sup>13</sup>C NMR (Fig. 1B), and FT-IR (Fig. 1C) analyses confirmed the successful synthesis of L-Cys NCA with high purity. The NH signal at 9.28 ppm (<sup>1</sup>H NMR) and two typical C=O stretching absorptions at 1852 and 1820  $\text{cm}^{-1}$  (FT-IR) indicated the formation of NCA ring. The <sup>13</sup>C NMR spectrum (Fig. 1B) also confirmed the L-Cys NCA structure. The signals at 170.09 and 151.78 ppm were assigned to the carboxyl groups in the NCA ring.

Based on the results of elemental analyses of the obtained PEG-poly(amino acid)s star copolymers, the molar ratios of mPEG/L-Cys/L-Phe were calculated and listed in Table 1. The chemical structures were further confirmed by <sup>1</sup>H NMR (Fig. 2A) and FT-IR (Fig. 2B). As shown in Fig. 2A, the <sup>1</sup>H NMR spectra showed resonances at 6.97 ppm (e), which were the characteristic signals of benzene ring protons on the L-phenylalanine units ( $\text{C}_6\text{H}_5$ , 5H). The resonances at 5.11–4.12



**Fig. 1** <sup>1</sup>H NMR (in DMSO-*d*<sub>6</sub>) (A), <sup>13</sup>C NMR (in DMSO-*d*<sub>6</sub>) (B), and FT-IR (C) spectra of L-Cys NCA.

(c + f) were assigned to the protons of the poly(amino acid) backbone ( $-\text{C}(\text{O})\text{CH}(\text{CH}_2\text{C}_6\text{H}_5)\text{NH}-$ , 1H and  $-\text{C}(\text{O})\text{CH}(\text{CH}_2\text{S}-)\text{NH}-$ , 1H). The resonances at 3.62 (b) and 3.28 (a) were attributed to the methylene protons and end methoxyl protons of mPEG ( $-\text{CH}_2\text{CH}_2-$ , 4H and  $\text{CH}_3-$ , 3H), respectively. The methylene protons of the poly(amino acid) side groups gave characteristic signals at 3.04–2.93 (d + g) ( $\text{C}_6\text{H}_5\text{CH}_2-$ , 2H and  $-\text{SCH}_2-$ , 2H). It must be noted that signals from the protons of the poly(amino acid) core were significantly suppressed in their

<sup>1</sup>H NMR spectra. It can be reasonably explained that highly cross-linked poly(amino acid) cores have less mobility, leading to decreased and broadened NMR signals. Similar phenomena have also been observed for PEG-polyphosphoester NG by Wang *et al.*,<sup>11,34</sup> and core-cross-linked miktoarm star copolymers by Matyjaszewski *et al.*<sup>35</sup> The FT-IR spectra (Fig. 2B) were also in agreement with the chemical structure of PEG-poly(amino acid)s, showing typical absorptions at 1659 ( $\nu_{\text{C}=\text{O}}$ ) and 1520 ( $\nu_{\text{C}(\text{O})-\text{NH}}$ )  $\text{cm}^{-1}$  attributed to the amide bond on the poly(amino acid) backbone and 1108 ( $\nu_{\text{C}-\text{O}-\text{C}}$ )  $\text{cm}^{-1}$  assigned to the ether bond of mPEG.

Amphiphilic polymers are capable of providing various self-assembled structures in the selective solvents.<sup>36,37</sup> In this work, the NGs were prepared by directly dispersing the disulfide-core-cross-linked PEG-poly(amino acid)s star copolymers in PBS at pH 7.4. Transmission electron microscopy (TEM) micrographs (Fig. 3A–C) showed that NG-1, -2 and -3 (Table 1) all took clear core-shell spherical morphology with the respective average diameters around 46, 84 and 143 nm. In contrast, the hydrodynamic radii ( $R_h$ ) measured by DLS were 168, 193, and 234 nm (Table 1). The smaller values from TEM observations should be due to the dehydration of the NGs in the TEM sample preparation process. To further determine whether the poly(amino acid) cores were cross-linked, we measured the fluorescence spectra of the pyrene probe in presence of different concentrations of the PEG-poly(amino acid)s. The excitation spectra of pyrene shows a significant blue shift when the pyrene molecules transfer from the hydrophobic domain to the hydrophilic domain or a water environment ( $\lambda_{\text{em}} = 390 \text{ nm}$ ).<sup>9,38</sup> In this work, no blue shift of absorption band was observed when the concentration of PEG-poly(amino acid)s was decreased from  $0.25$  to  $1.53 \times 10^{-5} \text{ g L}^{-1}$  in PBS at pH 7.4, as shown in Fig. S2 of the ESI.† This result suggested that the NG was not dissociated even at the concentration of  $1.53 \times 10^{-5} \text{ g L}^{-1}$ , indicating the stable cross-linked structure.

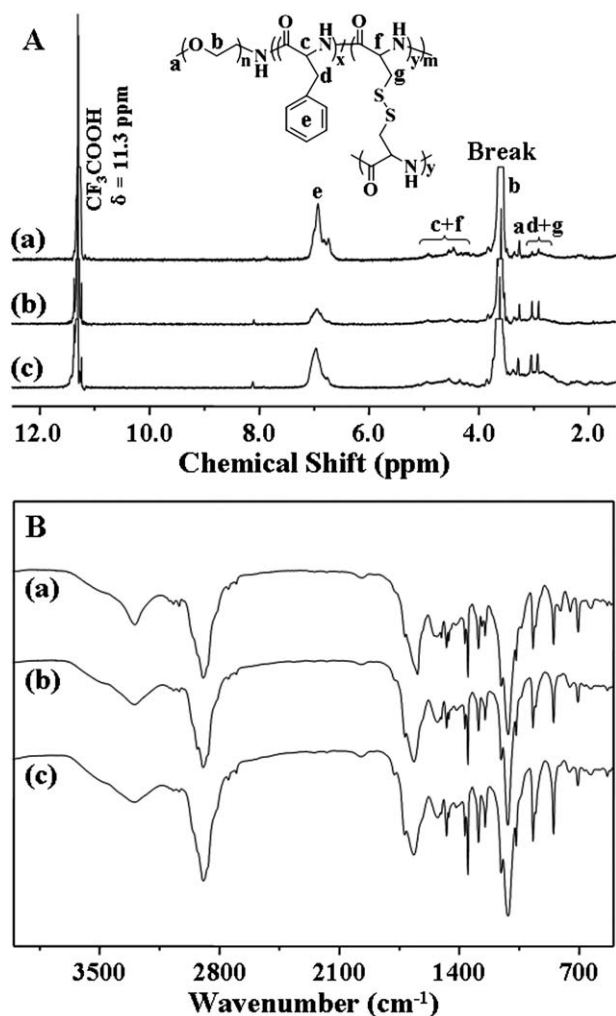
A reductive condition mimicking the intracellular circumstance was employed to check whether the NG could be de-cross-linked. The change of NG-1 size in response to 10 mM GSH was monitored over time in PBS (pH 7.4) at a concentration of  $0.1 \text{ g L}^{-1}$ . As shown in Fig. 4, the  $R_h$  of NG-1 increased from  $168 \pm 7.9$  to  $205 \pm 6.1 \text{ nm}$  slowly in the test duration (24 h). The phenomenon may be attributed to the decrease of the cross-linking density due to the cleavage of disulfide bonds.

#### *In vitro* DOX loading and reduction triggered drug release

DOX, an anthracycline anticancer drug, is widely used to treat different types of solid malignant tumors, which interacts with DNA through insertion and then inhibits the biosynthesis of bioactive macromolecules.<sup>39–41</sup> In this study, DOX was used as a model drug and loaded into the reduction-responsive NGs through dialysis method. As shown in Table 1, the DLC% of NG-1, -2 and -3 were 2.86, 8.64 and 12.34, depending on the compositions of NGs, while the DLE% were 14.72, 47.29 and 70.39, respectively. Comparison of the DLC% and DLE% of NGs indicated that higher DLC% and DLE% were attributed to the higher content of poly(amino acid)s as well as proportion of L-Cys in these systems. The increase in content of the poly(amino acid)s gained larger NG core, and the higher proportion of L-Cys

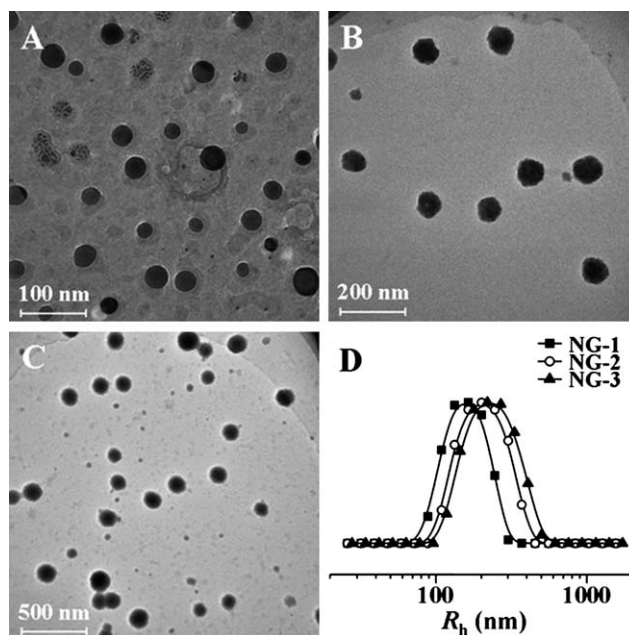
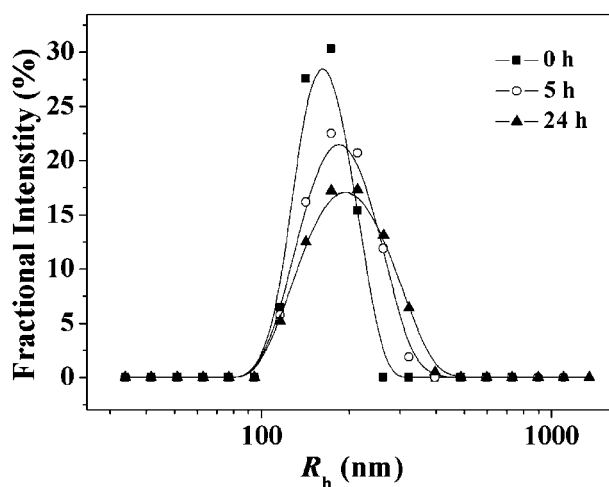
**Table 1** Characterization of PEG-poly(amino acid)s NGs

Entry	Feeding molar ratio of mPEG-NH <sub>2</sub> /L-Cys NCA/L-Phe NCA	Resultant molar ratio of mPEG/L-Cys/L-Phe <sup>a</sup>	R <sub>h</sub> (nm)	DLC (%)	DLE (%)
NG-1	1/3/22	1/2/19	168 ± 7.9	2.86	14.72
NG-2	1/6/22	1/6/23	193 ± 4.8	8.64	47.29
NG-3	1/9/33	1/9/32	234 ± 4.1	12.34	70.39

<sup>a</sup> Calculated by elemental analysis.**Fig. 2** <sup>1</sup>H NMR (in CF<sub>3</sub>COOD) (A), and FT-IR (B) spectra of NG-1 (a), NG-2 (b), NG-3 (c).

resulted in the more compact NG core, which are both effective to improve the DOX capture.

The drug release behaviors of the NGs with different contents and compositions of poly(amino acid)s were investigated with and without GSH at pH 7.4. The cumulative release percentages of DOX loaded in NGs *versus* time were plotted in Fig. 5. In the absence of GSH, less than 20% loaded DOX was released from the NGs in the test duration (93.5 h). However, the DOX release rates were accelerated by the presence of GSH and over 90% loaded DOX was released with 10 mM GSH, analogous to the intracellular reductive environment, in 93.5 h. The GSH concentration,

**Fig. 3** TEM micrographs of NG-1 (A), NG-2 (B) and NG-3 (C), and hydrodynamic radii ( $R_h$ ) of NGs (D).**Fig. 4** Change in the particle size ( $R_h$ ) of NG-1 in PBS at pH 7.4 in response to 10 mM GSH monitored by DLS.

and content and composition of poly(amino acid)s were found to be relevant to the drug release kinetics, and the release rates of DOX from NGs were in the order of NG-1 (10 mM GSH) > NG-2



**Fig. 5** *In vitro* release of DOX from DOX-loaded NG-1 (a), NG-2 (b) and NG-3 (c) without GSH, NG-3 with 2.5 (d) and 5 (e) mM GSH, and NG-1 (f), NG-2 (g) and NG-3 (h) with 10 mM GSH in PBS at pH 7.4, 37 °C. Data were presented as the average  $\pm$  standard deviation ( $n = 3$ ).

(10 mM GSH) > NG-3 (10 mM GSH) > NG-3 (5 mM GSH) > NG-3 (2.5 mM GSH) > NG-1, -2 and -3 (0 mM GSH). The fast DOX release from the NGs under the reductive condition was

most likely due to the swelling of the NGs during the cleavage of the disulfide bonds. Based on the results, we could conclude that the release rate of DOX from NGs could be affected by the content of poly(amino acid)s and the proportion of L-Cys. The increase in content of the poly(amino acid)s and the proportion of L-Cys led to the decrease DOX release rate from the NGs. Therefore, it was possible to modulate the release rate of DOX from the NGs by adjusting the GSH concentration, and poly(amino acid)s content and composition. These release profiles are not only beneficial for minimizing drug loss in circulation, but also for selective accumulation in tumor tissue by the enhanced permeability and retention (EPR) effect, which may enhance the overall therapeutic efficacy *in vivo*.

#### Intracellular DOX release

The cellular uptake and intracellular release behaviors of DOX-loaded NG towards HeLa cells were monitored by CLSM to determine whether the reduction-responsive NG was effective to deliver DOX into the cells. HeLa cells were first pretreated with 10 mM GSH for 2 h to improve the intracellular concentration of GSH uniformly and then incubated with DOX-loaded NGs for 0.5 or 2 h (10 mg L<sup>-1</sup> DOX). HeLa cells without GSH pretreatment were used as control. As expected, the stronger



**Fig. 6** Representative CLSM images of HeLa cells incubated with DOX-loaded NG-3: 0.5 h, cells without pretreatment (A) and pretreated with 10 mM GSH (B), and 2.0 h, cells without pretreatment (C) and pretreated with 10 mM GSH (D). For each panel, the images from left to right show differential interference contrast (DIC) images, cell nuclei stained by DAPI (blue), DOX fluorescence in cells (red), and overlays of the three images. The bar represents 20  $\mu$ m.

intracellular DOX fluorescence in GSH pretreated cells was observed after both 0.5 and 2 h incubation with DOX-loaded NG (Fig. 6). Several researchers including us have reported that the free DOX have stronger fluorescence compared with the DOX in the nanoparticles at the same concentration due to the self-quenching effect of DOX.<sup>9,22,42</sup> Thus, the enhanced fluorescence intensity in the GSH pretreated HeLa cells should be the result of the high endocytosis efficiency of DOX-loaded NG and enhanced intracellular release of DOX with NG degradation.

### *In vitro* cytotoxicities of NGs and DOX-loaded NG

The *in vitro* cytotoxicities of NGs and DOX-loaded NG toward HeLa cells were evaluated using MTT assays. As shown in Fig. 7A, the viabilities of HeLa cells treated with NGs for 24 h were around 85 to 100% at all test concentrations up to 50 mg L<sup>-1</sup>, revealing the low toxicity and good compatibility of the NGs to cells and rendering their potential as an efficient drug delivery vehicle.

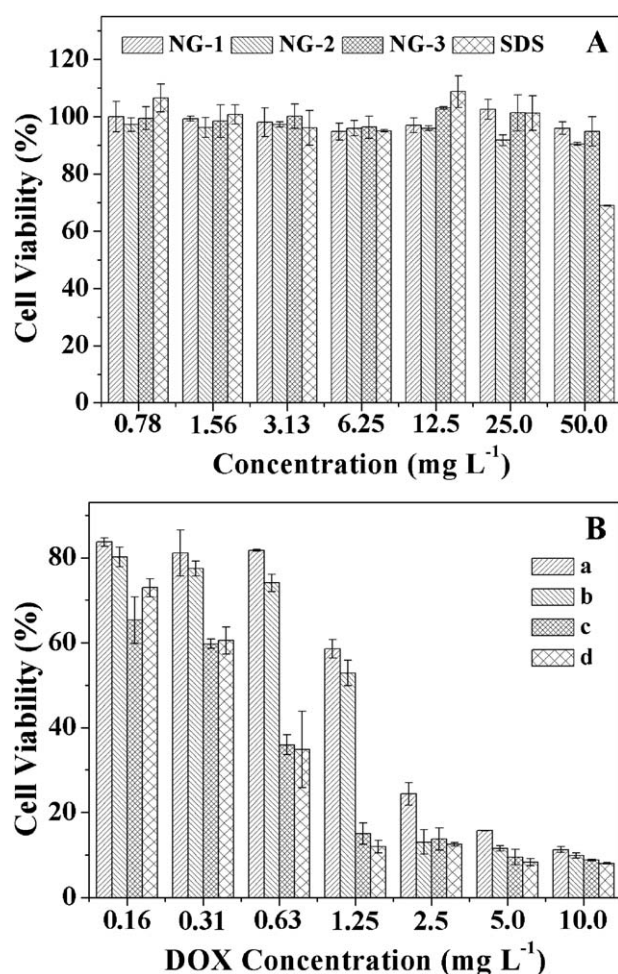


**Fig. 7** *In vitro* cytotoxicities of NGs to HeLa cells with SDS as positive control (A), the cytotoxicities of non-pretreated (a) and 10 mM GSH pretreated (b) HeLa cells after 24 h incubation with DOX-loaded NG-3 and the cytotoxicities of non-pretreated (c) and 10 mM GSH pretreated (d) HeLa cells after 24 h incubation with free DOX were used as the control (B). Data were presented as the average  $\pm$  standard deviation ( $n = 6$ ).

To determine the inhibition of HeLa cells proliferation *in vitro*, the cell viabilities of non-pretreated or 10 mM GSH pretreated HeLa cells were evaluated after 24 h incubation with DOX-loaded NG-3, and the cytotoxicities of non-pretreated and 10 mM GSH pretreated HeLa cells after 24 h incubation with free DOX were used as controls. As shown in Fig. 7B, the DOX-loaded NG exhibited higher inhibition efficacy to HeLa cells pretreated with GSH than that to non-pretreated cells, while in controls, the proliferation of HeLa cells incubated with free DOX was not affected by the pretreatment of GSH. The results revealed that the faster DOX release from NGs triggered by the higher intracellular GSH concentration, which enhanced the inhibition of the cell proliferation.

### Conclusions

A series of novel reduction-responsive disulfide-core-cross-linked PEG-poly(amino acid)s star copolymers were prepared through one-step ROP of L-Phe NCA and L-Cys NCA with mPEG-NH<sub>2</sub> as macroinitiator. The NGs were prepared by directly dispersing the obtained PEG-poly(amino acid)s in PBS at pH 7.4. DOX was loaded into NGs, and the release behaviors of DOX from DOX-loaded NGs could be regulated by the GSH concentration, and poly(amino acid)s content and composition. The higher GSH concentration, and lower poly(amino acid)s content and L-Cys proportion resulted in the faster DOX release. Moreover, the intracellular DOX release monitored by CLSM displayed that the faster intracellular release of DOX from NG occurred in GSH pretreated HeLa cells than that of non-pretreated cells. In addition, *in vitro* cell viability evaluation revealed that the NGs were biocompatible, and the cleavage of disulfide bonds triggered by intracellular GSH could accelerate the intracellular DOX release and thus enhance the *in vitro* cell proliferation inhibition. With convenient fabrication, good biocompatibility, stability in the circulation condition and accelerated intracellular drug release, the reduction-responsive NGs hold great promise for efficient intracellular delivery of potent anticancer drugs affording enhanced cancer therapy with fewer side effects.

### Acknowledgements

This work was supported by grants from National Natural Science Foundation of China (Key Project 50733003, Project 20904053, 51003103 and 50973108), Ministry of Science and Technology of China (International Cooperation and Communication Program 2010DFB50890), Scientific Development Program of Jilin Province (Project 20090135 and 201101082), Knowledge Innovation Program of the Chinese Academy of Sciences (Grant No. KJCX2-YW-H19). We would like to thank Prof. Joydeep Dutta from Disha Institute of Management and Technology for the valuable discussion.

### Notes and references

- 1 Y. L. Li, L. Zhu, Z. Z. Liu, R. Cheng, F. H. Meng, J. H. Cui, S. J. Ji and Z. Y. Zhong, *Angew. Chem., Int. Ed.*, 2009, **48**, 9914–9918.
- 2 J. Y. Liu, Y. Pang, W. Huang, X. H. Huang, L. L. Meng, X. Y. Zhu, Y. F. Zhou and D. Y. Yan, *Biomacromolecules*, 2011, **12**, 1567–1577.
- 3 L. Y. Tang, Y. C. Wang, Y. Li, J. Z. Du and J. Wang, *Bioconjugate Chem.*, 2009, **20**, 1095–1099.

- 4 M. Campillos, M. Kuhn, A. C. Gavin, L. J. Jensen and P. Bork, *Science*, 2008, **321**, 263–266.
- 5 A. N. Koo, H. J. Lee, S. E. Kim, J. H. Chang, C. Park, C. Kim, J. H. Park and S. C. Lee, *Chem. Commun.*, 2008, 6570–6572.
- 6 Y. Pang, J. Y. Liu, Y. Su, J. L. Wu, L. J. Zhu, X. Y. Zhu, D. Y. Yan and B. S. Zhu, *Polym. Chem.*, 2011, **2**, 1661–1670.
- 7 W. Wang, J. Ding, C. Xiao, Z. Tang, D. Li, J. Chen, X. Zhuang and X. Chen, *Biomacromolecules*, 2011, **12**, 2466–2474.
- 8 C. J. F. Rijcken, O. Soga, W. E. Hennink and C. F. van Nostrum, *J. Controlled Release*, 2007, **120**, 131–148.
- 9 K. Wang, H. Q. Dong, H. Y. Wen, M. Xu, C. Li, Y. Y. Li, H. N. Jones, D. L. Shi and X. Z. Zhang, *Macromol. Biosci.*, 2011, **11**, 65–71.
- 10 E. Kluza, S. Y. Yeo, S. Schmid, D. W. J. Van der Schaft, R. W. Boekhoven, R. M. Schiffelers, G. Storm, G. J. Strijkers and K. Nicolay, *J. Controlled Release*, 2011, **151**, 10–17.
- 11 M. H. Xiong, J. Wu, Y. C. Wang, L. S. Li, X. B. Liu, G. Z. Zhang, L. F. Yan and J. Wang, *Macromolecules*, 2009, **42**, 893–896.
- 12 S. E. Averick, A. J. D. Magenau, A. Simakova, B. F. Woodman, A. Seong, R. A. Mehl and K. Matyjaszewski, *Polym. Chem.*, 2011, **2**, 1476–1478.
- 13 J. Ferreira, J. Syrett, M. Whittaker, D. Haddleton, T. P. Davis and C. Boyer, *Polym. Chem.*, 2011, **2**, 1671–1677.
- 14 T. Xing, B. Lai, X. Ye and L. Yan, *Macromol. Biosci.*, 2011, **11**, 962–969.
- 15 J. Ding, X. Zhuang, C. Xiao, Y. Cheng, L. Zhao, C. He, Z. Tang and X. Chen, *J. Mater. Chem.*, 2011, **21**, 11383–11391.
- 16 D. B. Hua, J. L. Jiang, L. J. Kuang, J. Jiang, W. Zheng and H. J. Liang, *Macromolecules*, 2011, **44**, 1298–1302.
- 17 S. J. Lee, K. H. Min, H. J. Lee, A. N. Koo, H. P. Rim, B. J. Jeon, S. Y. Jeong, J. S. Heo and S. C. Lee, *Biomacromolecules*, 2011, **12**, 1224–1233.
- 18 L. Y. Zhang, R. Guo, M. Yang, X. Q. Jiang and B. R. Liu, *Adv. Mater.*, 2007, **19**, 2988–2992.
- 19 J. Z. Du, T. M. Sun, W. J. Song, J. Wu and J. Wang, *Angew. Chem., Int. Ed.*, 2010, **49**, 3621–3626.
- 20 L. J. Wong, M. Kavallaris and V. Bulmus, *Polym. Chem.*, 2011, **2**, 385–393.
- 21 N. Ma, Y. Li, H. P. Xu, Z. Q. Wang and X. Zhang, *J. Am. Chem. Soc.*, 2010, **132**, 442–443.
- 22 Y. C. Wang, Y. Li, T. M. Sun, M. H. Xiong, J. A. Wu, Y. Y. Yang and J. Wang, *Macromol. Rapid Commun.*, 2010, **31**, 1201–1206.
- 23 T. B. Ren, Y. Feng, Z. H. Zhang, L. Li and Y. Y. Li, *Soft Matter*, 2011, **7**, 2329–2331.
- 24 P. D. Thornton, R. J. Mart and R. V. Ulijn, *Adv. Mater.*, 2007, **19**, 1252–1256.
- 25 A. Russo, W. Degraff, N. Friedman and J. B. Mitchell, *Cancer Res.*, 1986, **46**, 2845–2848.
- 26 N. V. Nukolova, H. S. Oberoi, S. M. Cohen, A. V. Kabanov and T. K. Bronich, *Biomaterials*, 2011, **32**, 5417–5426.
- 27 J. H. Ryu, R. T. Chacko, S. Jiwpanich, S. Bickerton, R. P. Babu and S. Thayumanavan, *J. Am. Chem. Soc.*, 2010, **132**, 17227–17235.
- 28 J. X. Ding, C. S. Xiao, L. Zhao, Y. L. Cheng, L. L. Ma, Z. H. Tang, X. L. Zhuang and X. S. Chen, *J. Polym. Sci., Part A: Polym. Chem.*, 2011, **49**, 2665–2676.
- 29 J. Ding, C. Xiao, Z. Tang, X. Zhuang and X. Chen, *Macromol. Biosci.*, 2011, **11**, 192–198.
- 30 J. Sun, X. S. Chen, C. Deng, H. J. Yu, Z. G. Xie and X. B. Jing, *Langmuir*, 2007, **23**, 8308–8315.
- 31 M. S. Thompson, T. P. Vadala, M. L. Vadala, Y. Lin and J. S. Riffle, *Polymer*, 2008, **49**, 345–373.
- 32 A. C. Engler, H. I. Lee and P. T. Hammond, *Angew. Chem., Int. Ed.*, 2009, **48**, 9334–9338.
- 33 N. Hadjichristidis, H. Iatrou, M. Pitsikalis and G. Sakellariou, *Chem. Rev.*, 2009, **109**, 5528–5578.
- 34 J. Wu, X. Q. Liu, Y. C. Wang and J. Wang, *J. Mater. Chem.*, 2009, **19**, 7856–7863.
- 35 H. F. Gao, N. V. Tsarevsky and K. Matyjaszewski, *Macromolecules*, 2005, **38**, 5995–6004.
- 36 M. C. Jones and J. C. Leroux, *Soft Matter*, 2010, **6**, 5850–5859.
- 37 Y. C. Wang, S. Y. Shen, Q. P. Wu, D. P. Chen, J. Wang, G. Steinhoff and N. Ma, *Macromolecules*, 2006, **39**, 8992–8998.
- 38 J. Cheng, J. X. Ding, Y. C. Wang and J. Wang, *Polymer*, 2008, **49**, 4784–4790.
- 39 D. A. Gewirtz, *Biochem. Pharmacol.*, 1999, **57**, 727–741.
- 40 Y. G. Wang, T. Y. Yang, X. Wang, W. B. Dai, J. C. Wang, X. A. Zhang, Z. Q. Li and Q. A. Zhang, *J. Controlled Release*, 2011, **149**, 299–306.
- 41 L. Zhou, R. Cheng, H. Q. Tao, S. B. Ma, W. W. Guo, F. H. Meng, H. Y. Liu, Z. Liu and Z. Y. Zhong, *Biomacromolecules*, 2011, **12**, 1460–1467.
- 42 H. L. Sun, B. N. Guo, R. Cheng, F. H. Meng, H. Y. Liu and Z. Y. Zhong, *Biomaterials*, 2009, **30**, 6358–6366.